Received: 8 April 2020 | Accepted: 21 May 2020

DOI: 10.1111/jth.14940

ORIGINAL ARTICLE

Development and characterization of single-domain antibodies neutralizing protease nexin-1 as tools to increase thrombin generation

Charlotte Kawecki[1,2] | Karen Aymonnier[2] | Stephen Ferrière[1] | Laurence Venisse[2] | Véronique Arocas[2] | Yacine Boulaftali[2] | Olivier D. Christophe[1] | Peter J. Lenting[1] | Marie-Christine Bouton[2] | Cécile V. Denis[1]

[1]Institut National de la Santé et de la Recherche Médicale, UMR_S 1176, Université Paris-Saclay, Le Kremlin-Bicêtre, France

[2]Institut National de la Santé et de la Recherche Médicale, UMR_S 1148, Université de Paris, Paris, France

Correspondence
Cécile V. Denis, INSERM U1176, 80 rue du General Leclerc, 94276 Le Kremlin-Bicêtre cedex, France.
Email: cecile.denis@inserm.fr

Funding information
Société Française d'Hématologie; Agence Nationale de la Recherche, Grant/Award Number: ANR-14-OHRI-0013

Abstract

Background: Protease nexin-1 (PN-1) is a member of the serine protease inhibitor (Serpin)-family, with thrombin as its main target. Current polyclonal and monoclonal antibodies against PN-1 frequently cross-react with plasminogen activator inhibitor-1 (PAI-1), a structurally and functionally homologous Serpin.

Objectives: Here, we aimed to develop inhibitory single-domain antibodies (VHHs) that show specific binding to both human (hPN-1) and murine (mPN-1) PN-1.

Methods: PN-1-binding VHHs were isolated via phage-display using llama-derived or synthetic VHH-libraries. Following bacterial expression, purified VHHs were analyzed in binding and activity assays.

Results and Conclusions: By using a llama-derived library, 2 PN-1 specific VHHs were obtained (KB-PN1-01 and KB-PN1-02). Despite their specificity, none displayed inhibitory activity toward hPN-1 or mPN-1. From the synthetic library, 4 VHHs (H12, B11, F06, A08) could be isolated that combined efficient binding to both hPN-1 and mPN-1 with negligible binding to PAI-1. Of these, B11, F06, and A08 were able to fully restore thrombin activity by blocking PN-1. As monovalent VHH, half-maximal inhibitory concentration values for hPN-1 were 50 ± 10, 290 ± 30, and 960 ± 390 nmol/L, for B11, F06, and A08, respectively, and 1580 ± 240, 560 ± 130, and 2880 ± 770 nmol/L for mPN-1. The inhibitory potential was improved 4- to 7-fold when bivalent VHHs were engineered. Importantly, all VHHs could block PN-1 activity in plasma as well as PN-1 released from activated platelets, one of the main sources of PN-1 during hemostasis. In conclusion, we report the generation of inhibitory anti-PN-1 antibodies using a specific approach to avoid cross-reactivity with the homologous Serpin PAI-1.

KEYWORDS

phage display, protease nexin-1, serpin, single-domain antibody, thrombin

Kawecki and Aymonnier equal contribution.

Manuscript handled by: James Morrissey

Final decision: James Morrissey, 21 May 2020

1 | INTRODUCTION

Protease nexin-1 (PN-1) belongs to a family of structurally related proteins known as inhibitors of serine protease or serpins, which can be found in most organisms.[1] Serpins use their reactive center loops (RCL) to target the active site of serine proteases, driving the complex into a suicide substrate inhibition mechanism. This leads to inactivation of the protease and often rapid clearance via scavenger receptors.

Phylogenetically, PN-1 is most closely related to plasminogen activator inhibitor 1 (PAI-1) with 41% shared sequence.[2] PN-1 is undetectable in the circulating blood, but is present in circulating cells (monocytes and platelets) and vascular cells.[3] PN-1 is secreted during platelet activation and efficiently inhibits thrombin, the key enzyme of the coagulation cascade which catalyzes fibrin formation.[4] Besides thrombin, PN-1 inhibits several other serine proteases, albeit much less efficiently, such as trypsin, tissue-type plasminogen activator, urokinase-type plasminogen activator (u-PA), plasmin, factor Xa, factor XIa, activated protein C, and factor VII activating protease.[5-9] Its physiological role extends to several processes, like coagulation, fibrinolysis and tissue remodelling.[3,4,10]

Recently, we have investigated the impact of PN-1 inhibition on coagulation in both mice and patients with hemophilia. Interestingly, polyclonal antibody-mediated inhibition of PN-1 in hemophilic patient plasma led to an increase of thrombin generation and of clot strength, as well as a reduction of fibrinolysis. Furthermore, the bleeding phenotype of hemophilic mice is mitigated by PN-1 deficiency. Inhibition of PN-1 could thus potentially be used to restore the hemostatic balance between pro- and anticoagulant systems in hemophilia.[11] This observation is in line with current developments of new therapeutics in the hemophilia field, which aim for restoring this balance by neutralizing natural anticoagulants: targeting of antithrombin expression by small interfering RNA, of tissue factor pathway inhibitor by antibodies, or of activated protein C by an engineered serpin are all strategies under investigation.[12-14]

Currently, there is a lack of specific anti-PN-1 antibodies that could block PN-1 function. Very few monoclonal and polyclonal inhibitory anti-PN-1 antibodies are available, and many of them (including those that are commercially available) cross-react with the closest PN-1 family member, PAI-1. We therefore chose to develop single domain-antibodies (VHHs) targeting PN-1. VHHs have many inherent, advantageous properties, such as their low molecular mass (15 kDa), low immunogenicity, high affinity, high solubility and stability, and easy production in bacteria.[15-17] In comparison with classical immunoglobulins, VHHs display hypervariable complementary determining regions (CDRs), which can recognize specific epitopes that are less accessible, or buried deep in structural clefts.[18] Furthermore, VHHs are often potent inhibitors of proteins because of their long CDR3 domain, which is able to penetrate into the catalytic cleft of enzymes.[19] Taken together, these characteristics led us to hypothesize that the generation of inhibitory VHHs against PN-1 could generate new tools to study the impact of PN-1 inhibition in hemostasis. We report the isolation of three specific inhibitory VHHs against PN-1.

Essentials

- Protease nexin-1 (PN-1) belongs to the serpin-family and is an inhibitor of thrombin.
- Most antibodies targeting PN-1 cross-react with plasminogen activator inhibitor-1.
- We isolated single-domain antibodies (VHHs) that specifically bind and neutralize PN-1.
- These VHHs represent novel tools to study the biology and the functions of PN-1.

2 | MATERIALS AND METHODS

2.1 | Materials

Isopropyl β-D-1-thiogalactopyranoside (IPTG), human serum albumin (HSA), bovine serum albumin (BSA) were from Sigma-Aldrich (Saint-Quentin Fallavier, France). Polyclonal rabbit anti-cMyc tag peroxidase-labelled, polyclonal rabbit anti-6xHis-tag antibodies were from Abcam (Paris, France). Human and murine PN-1 and human α-thrombin were prepared as described previously.[20,21] Prothrombin time (PT) and activated partial thromboplastin time (aPTT) reagents were from Stago-Diagnostica (Asnières-sur-Seine, France). Chromogenic substrates PNAPEP-1344 and PNAPEP-0238 were from Cryopep (Montpellier, France). Dynabeads M-450 epoxy beads, *E coli* TG1 cells, Terrific Broth (TB) medium, Lysogeny Broth medium were from ThermoFisher Scientific (Villebon-sur-Yvette, France). PAI-1 was from Stago BNL (Lille, France). 4-(2-aminoethyl) benzenesulfonyl fluoride hydrochloride was from vWR (Fontenay-sous-Bois, France).

2.2 | Construction of anti-PN-1 VHHs from lymphocytes library by phage display

Immunization of a single llama (*L. glama*) was outsourced to the Centre de Recherche en Cancérologie (Université Aix-Marseille, Marseille, France).[22] Briefly, the llama was immunized with 100 μg of a mix of human or murine PN-1 in equal proportion with Freund's incomplete adjuvant. After blood sampling, messenger RNA was extracted from lymphocytes and the VHH library was constructed as described.[22-24] The library contains VHH-coding DNA fragments, which were cloned into the pHEN6-phagemid vector and transformed in electrocompetent *E coli* TG1 cells[25] (ThermoFisher Scientific) to generate a library of 0.9×10^8 clones. The M13K07 phage helper was used to infect the TG1 VHH library to allow surface expression of the VHHs.

2.3 | Negative and positive selection of VHHs

To reduce the number of VHHs cross-reacting with PAI-1, phage particles were first incubated with beads coated with 100 μg PAI-1 (1 hour at room temperature in phosphate-buffered saline [PBS]-3% BSA). Nonbinding phages were passed on beads coated with a mixture of murine PN-1 and human PN-1 (50 μg of each). Captured phages were eluted with 0.5 mg/mL trypsin. Three consecutive rounds of enrichment were performed.

2.4 | Selection of anti-PN1-specific VHHs

After infection of TG1 bacteria with isolated phages, cells were grown 4 hours under agitation in TB medium, then 1 mmol/L IPTG was added to induce VHH expression at 30°C. Eighteen hours after induction, cells were centrifuged and periplasmic extract was collected after lysis in TES buffer (200 mmol/L Tris-HCl, pH8, 0.5 mmol/L EDTA, and 500 mmol/L sucrose) for 1 hour at 4°C followed by 30 minutes with TES buffer diluted 4-fold in PBS. Released soluble proteins were tested for binding to PN-1, PAI-1, or BSA. Proteins (1 μg/well) were coated on NUNC Maxisorp-plates (ThermoFisher Scientific) in PBS overnight at 4°C. After saturation (PBS-BSA 3%, 1 hour at 37°C), bound VHHs were probed using alkaline phosphatase-coupled polyclonal anti-6xHis-tag antibody, detected via hydrolysis of 3,3′,5,5′-tetramethylbenzidine (TMB) and absorbance was read at 450 nm.

2.5 | Isolation of anti-PN-1 VHH from a synthetic library

In a second approach, a synthetic VHH library was used to isolate anti-PN-1 VHHs (Hybrigenics Services SAS, Paris, France). This hs-2dAb phage-display library containing 3×10^9 VHHs was first incubated with human PAI-1-coated beads to reduce unspecific binders. Unbound VHHs were then incubated with murine or human PN-1-coated beads. A total of three rounds of phage display were performed, with the depletion step being repeated during each round. After three rounds, 90 *E coli* clones were picked randomly and analyzed for binding to human and murine PN-1 as well as PAI-1. Phage-clones showing >5-fold increased signal to PN-1 over PAI-1 were considered as specific binders for PN-1 (mouse, human, or both). Sequencing of the positive clones revealed the presence of 18 different positive VHHs. Four of these recognized both mPN-1 and hPN-1, and were subcloned in the pHEN2-vector for further characterization.

2.6 | VHH subcloning, expression, and purification

Anti-PN-1 VHHs were transformed directly into *E coli* WK6 cells. Each clone was first grown in 10 mL LB-medium/100 μg/mL ampicillin/2% glucose/1 mmol/L $MgCl_2$ overnight at 37°C under gentle agitation. A total of 3 mL of this preculture was used to inoculate 330 mL of TB-medium/100 μg/mL ampicillin/0.1% glucose/1 mmol/L $MgCl_2$. The culture agitated (170 rpm, 37°C) until it reached an OD_{600} between 0.8 and 1. VHH expression was then induced by 1 mmol/L IPTG and the medium was left to grow overnight (170 rpm, 28°C). The periplasmic proteins were extracted by sonication (Fisher Scientific, Illkirch, France) during 30 minutes with a cycle 10 seconds ON/10 seconds OFF. The percentage of lysis was verified by a ratio (OD after lysis/OD before lysis) × 100. His-tagged VHHs were next purified via Co^{2+}-affinity chromatography as instructed (VWR). Minor contaminants were removed via size-exclusion chromatography using 20 mmol/L Hepes (pH 7.4)/0.1 M NaCl as equilibrium buffer. Purified VHHs displayed >95% homogeneity as assessed via sodium dodecyl sulfate–polyacrylamide gel electrophoresis and Coomassie staining.

For bivalent VHHs, two copies of monovalent single-domain antibodies (sdAbs) were separated by a linker consisting of $[GGGs]_3$ and a C-terminal 6xHis-Tag allowed for purification via Co^{2+}-affinity chromatography.

2.7 | hPAI-1 and mPAI-1 ELISA

Immulon 2-plates were coated with a murine monoclonal antibody to mPAI-1 or hPAI-1 (0.4 μg/well; Bio-Techne, Rennes, France) overnight at room temperature. After washing with PBS-tween-20 0.05%, wells were saturated with PBS-BSA 1%, 1 hour at room temperature. After washing, human or murine PAI-1 (2 pg/mL) were incubated for 2 hours at room temperature. Then, VHHs (10 μg/mL) were incubated 2 hours at room temperature. Bound VHHs were probed with a peroxidase-labelled polyclonal anti-6xHis-tag antibody and detected via hydrolysis of TMB and absorbance was read at 450 nm.

2.8 | hPN-1 and mPN-1 ELISA

Microlon-Med half-wells plates (Greiner bio-one, Courtaboeuf, France) were coated with 0.5 μg mPN-1 or hPN-1/well overnight at 4°C and then incubated with different concentrations of VHHs (0-20 μg/mL) in PBS/BSA 0.1%/Tween-20 0.1% for 2 hours at 37°C. Bound anti-PN-1 VHHs were probed with peroxidase-labelled polyclonal anti-cMyc tag antibody for monovalent VHHs or anti-6xHis-tag antibody for bivalent VHHs in the same buffer and detected via hydrolysis of TMB and absorbance was read at 450 nm.

2.9 | Inhibition of thrombin activity by PN-1

In a 96-well plate (Greiner Bio-one), various concentrations of anti-PN-1 VHHs were incubated with 10 nM PN-1 during 15 minutes at room temperature in 20 mmol/L Hepes/0.15 M NaCl/0.1% HSA. A total of 1 nmol/L purified thrombin was then added to the wells and incubated 30 minutes at room temperature. Thrombin activity

was quantified by measuring the rate of p-nitroaniline release from the chromogenic substrate H-D-Phe-Pip-Arg-pNA (PNAPEP-0238) (0.2 mmol/L), at 37°C, and read at 405 nm in a multiwell plate reader.

To calculate the half-maximal inhibitory concentration (IC50) of each VHH, a slightly modified protocol was used: anti-PN-1 VHHs were used at concentrations between 0 and 2 μmol/L, incubation of VHHs was performed during 5 minutes followed by 10 minutes' incubation with 1 nmol/L thrombin. PNAPEP-0238 substrate was added at a concentration of 0.2 mmol/L and incubated for 2 hours at 37°C. Quantification of thrombin activity was performed as described previously.

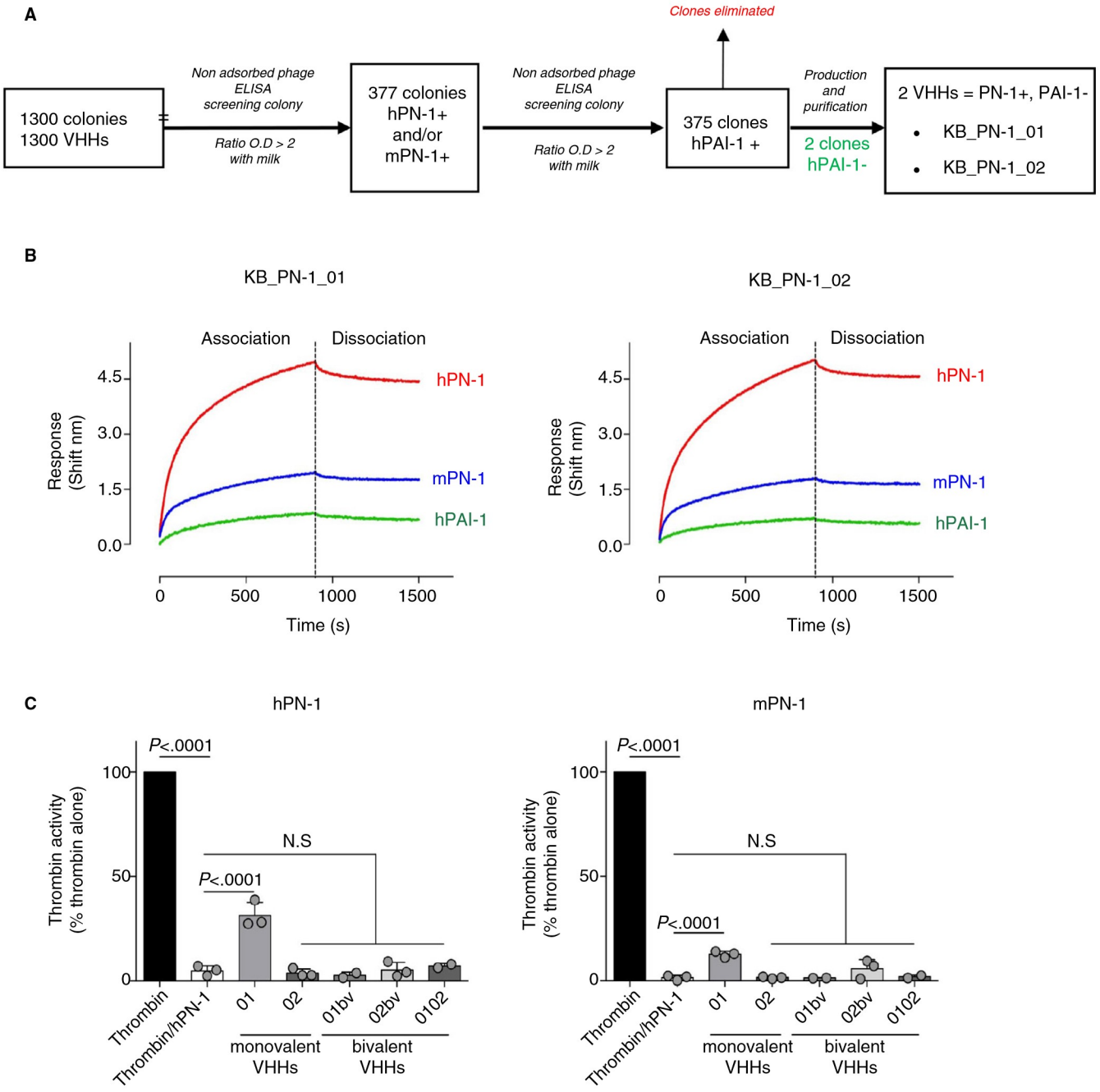

FIGURE 1 Identification and characterization of PN-1-specific VHHs by phage display. A, Summary of clone selection after three rounds of phage display leading to the identification of two specific PN-1 nanobodies named KB-PN1-01 and KB-PN1-02. B, Representative biolayer interferometry (BLI)-analysis graphs (Octet) of molecular binding between monovalent VHHs and hPN-1, mPN-1, or hPAI-1. Twenty-five μg/mL of monovalent VHHs were coated on the biosensor, and association with 1 μmol/L of hPN-1, mPN-1, or hPAI-1 were measured over an association phase of 900 s. Results are expressed as the wavelength shift (in nanometers) generated by the binding of the different molecules. C, Thrombin (1 nmol/L) was incubated with hPN-1 or mPN-1 (20 nmol/L), which were preincubated for 30 min in the absence or presence of monovalent or bivalent VHHs (20 μmol/L). Residual thrombin activity was measured by measuring the rate of PNAPEP-0238 hydrolysis. Data (mean ± SD; n = 3) represent residual thrombin activity as percentage of thrombin alone

2.10 | Inhibition thrombin activity by endogenous PN-1

Blood samples were taken in ACD-A anticoagulant tubes. Blood was centrifuged at 120*g* during 15 minutes to recover the platelet-rich plasma. Then, 2 µL/mL apyrase (5 mg/mL) and 1 µL/mL PGE1 (10 mmol/L) were added and the platelet-rich plasma was centrifuged at 1200*g*, 12 minutes at 20°C. The pellet was resuspended gently in washing buffer (3.6 mmol/L citric acid, 0.5 mmol/L glucose, 0.5 mmol/L KCl, 10.3 mmol/L NaCl, 2 mmol/L $CaCl_2$ pH6.5, 0.30% BSA, 2 µL/mL apyrase [5 mg/mL], and 1 µL/mL PGE1 [10 mmol/L]) and centrifuged 12 minutes at 1200*g* at 20°C. The platelets were adjusted to a concentration of 5×10^8 cells/mL in reaction buffer (0.03 mmol/L NaH2PO4, 0.5 mmol/L Hepes, 0.55 mmol/L glucose, 0.2 mmol/L $MgCl_2$, 0.1 mmol/L KCl, 13.7 mmol/L NaCl, 12 mmol/L $NaHCO_3$, 2 mmol/L $CaCl_2$, pH 7.3, and 0.3% BSA). For the condition "activated platelets," 50 µmol/L of thrombin receptor activating peptide (TRAP) was added to the platelets for 30 minutes at 37°C. Platelet were centrifuged 1200*g* for 10 minutes at room temperature to keep the supernatant.

In a 96-well plate (Greiner Bio-one), 80 µL of activated or non-activated platelets supernatant was spiked with 1 µmol/L of VHHs and incubated 15 minutes at room temperature. Then, 0.1 nmol/L of thrombin was added to each well and incubated for 30 minutes at room temperature. PNAPEP-0238 substrate was added at a concentration of 0.2 mmol/L and incubated for 2 hours at 37°C. Quantification of thrombin activity was performed as described previously.

2.11 | Inhibition of u-PA by human PAI-1

In a 96-well plate (Greiner Bio-one), 10 µmol/L anti-PN-1 VHHs were incubated with 10 nmol/L PAI-1 for 15 minutes at room temperature in 20 mmol/L Hepes pH7.5, 150 mmol/L NaCl, 0.1% HSA, and pH7.5. A total of 1.3 nmol/L of u-PA was subsequently added. After 10 minutes' incubation at room temperature, wells were quantified for u-PA activity by measuring the rate of p-nitroaniline release from the chromogenic substrate Glu-Gly-Arg-pNA, PNAPEP-1344 (0.2 mmol/L) at 37°C and read at 405 nm by a multiwell plate reader.

2.12 | Test of VHHs specificity by biolayer interferometry analysis

Equilibrium binding was performed via biolayer interferometry (BLI) analysis using Octet QK-equipment (Fortebio, Reading, UK). Monovalent VHHs (25 µg/mL) diluted in 100 mmol/L 2-(N-morpholino) ethanesulfonic acid (pH 5.0) were immobilized onto amine reactive biosensors. After quenching by ethanolamine, VHH-coated sensors were incubated with human or murine PN-1

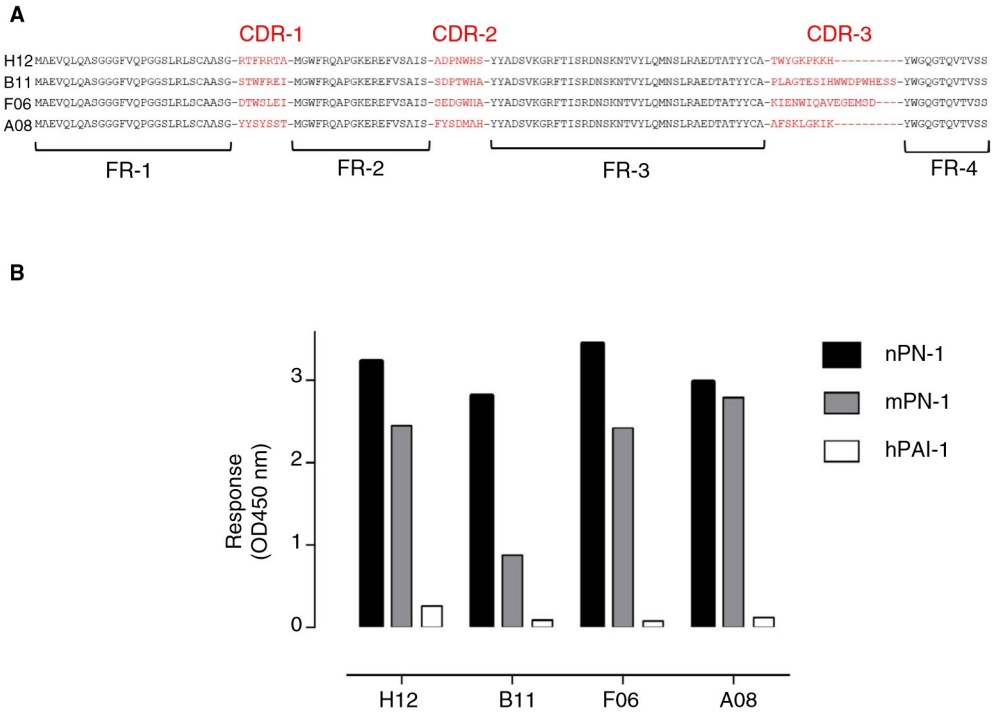

FIGURE 2 Identification and sequences of sdAbs isolated from a synthetic library. A, Amino acid sequences of four sdAbs with the four conserved framework regions (FR) responsible for core structure of the immunoglobulin domain and the 3 hypervariable complementarity-determining regions (CDR) labelled in red involved in antigen binding. B, Nonadsorbed phage ELISA determining positive clones obtained after three rounds of phage display experiment. Phages were added to plates coated with hPN-1, mPN-1, or hPAI-1. An horseradish peroxidase-conjugated anti-M13 antibody and a colorimetric substrate were used to measure binding. VHH clones that showed a significant ELISA signal in the presence of mPN-1 and hPN-1 and a very low signal in the presence of hPAI-1 were considered specific

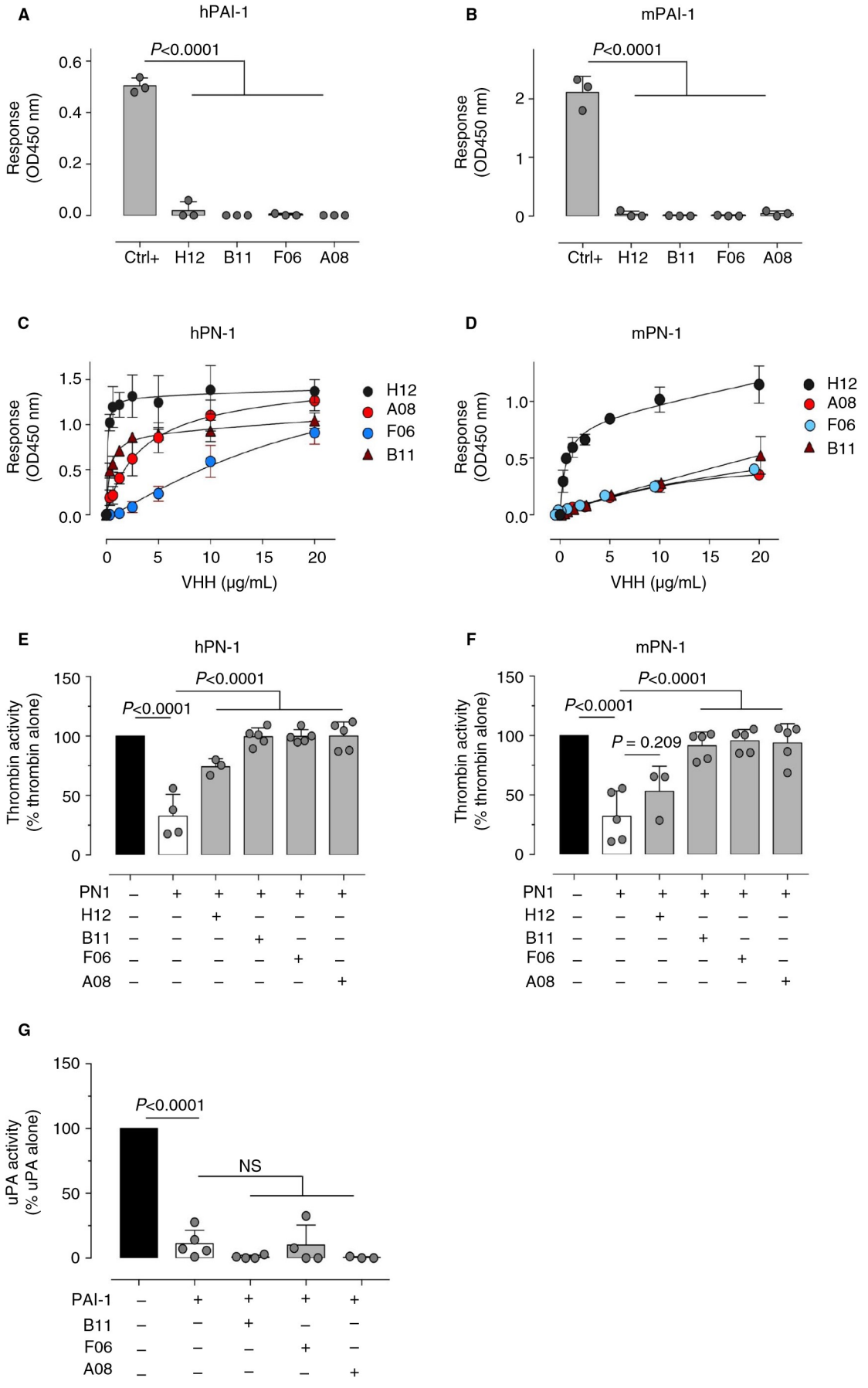

FIGURE 3 Characterization of VHHs obtained from a synthetic library. A-B, Wells coated with mAb anti-PAI-1 and 2 pg/mL of hPAI-1 (A) or mPAI-1 (B) were incubated with VHHs (10 μg/mL). Bound VHHs were probed with peroxidase-labelled pAb anti-6X-His tag. C-D, Wells were coated with 0.5 μg of hPN-1 (C) or mPN-1 (D) and incubated with different concentrations of monovalent VHHs (0.3-20 μg/mL). Bound VHHs were probed with peroxidase-labeled pAb-cMyc tag. E-F, One nanomole/liter of thrombin was incubated with 10 nmol/L hPN-1 (E) or mPN-1 (F) in the presence or absence of VHHs (10 μmol/L). Residual thrombin activity was measured by the rate of PNAPEP-0238-hydrolysis. Data (mean ± SD; n = 3-5) represent residual thrombin activity as percentage of thrombin alone. G, Urokinase plasminogen activator (u-PA; 1.3 nmol/L) was incubated with hPAI-1 (10 nmol/L) in the absence or presence of VHHs (10 μmol/L). Residual u-Pa activity was measured by the rate of PNAPEP-1344-hydrolysis. Data (n = 3-5) represent residual u-PA activity as percentage of u-PA alone

or human PAI-1 (1 μmol/L) in PBS-Tween 0.1% buffer for 15 minutes to allow association. Subsequently, biosensors were incubated in PBS-Tween 0.1% buffer for 10 minutes to initiate dissociation. In alternative experiments, 50 μg/mL biotinylated RCL of PN-1 was immobilized on streptavidin sensors in PBS- Tween 0.1% buffer. Before the association, 5 U of thrombin or buffer PBS-Tween were incubated with sensor during 30 minutes at 37°C then the association of bivalent VHHs (100 μg/mL) was followed for 15 minutes at 37°C. Subsequently, biosensors were put in PBS-Tween 0.1% buffer for 10 minutes to initiate dissociation. Data were analyzed using Octet Software, version 4.0.

2.13 | Modified prothrombin time

Fifty microliters of murine normal pooled plasma were diluted 8-fold in Owren-Koller buffer and 50 μL FII-deficient (prothrombin-deficient) lyophilized plasma (Stago-Diagnostica) were added. The mix was incubated 15 minutes at 37°C with 62.5 nmol/L of mPN-1 with or without 288 nmol/L bivalent VHHs. Prothrombin time was started by adding 100 μL Neoplastin CI (Stago-Diagnostica) to the mix. Clot formation was measured by coagulometer STArt (Stago-Diagnostica). Assays were performed three times in duplicate at 37°C.

2.14 | Modified activated partial thromboplastin time

Fifty microliters of FVIII-deficient murine plasma were diluted 8-fold in Owren-Koller buffer to which 50 μL of FVIII-deficient lyophilized plasma and 50 μL of PTT reagent (Stago-Diagnostica) were added. After a 100-second incubation, 625 nmol/L VHHs and 500 nmol/L mPN-1 were added. After 240 seconds of incubation at 37°C, the aPTT test was started by adding 100 μL 0.025 M $CaCl_2$. The clot formation was measured by a coagulometer. Assays were performed three times in duplicate at 37°C.

2.15 | Statistical analysis

Data are presented as mean with standard deviation (SD) and was analyzed using Prism software. One-way analysis of variance was used for values comparisons with control. *P* values <.05 and < .0001 were considered significant and highly significant, respectively.

3 | RESULTS

3.1 | Identification and characterization of VHHs obtained by llama immunization

The VHH library was obtained from messenger RNA of lymphocytes isolated 6 weeks after the first llama immunization. Phage display was used to select VHHs specific for PN-1. The selection has been performed in two steps: first, we selected negatively all VHHs that did not bind to magnetic beads coated with PAI-1 to reduce the number of anti-PAI-1 VHHs, whereas the second step consisted in elution of all VHHs bound to magnetic beads coated with PN-1. Such a two-step procedure was deemed necessary because PN-1 and PAI-1 contain conserved sequences.[26] After three rounds of phage display, we obtained 1300 VHHs that were subsequently screened (Figure 1A). a total of 377 VHHs (29%) recognized hPN-1 and/or mPN-1 above the previously defined threshold (OD at least twice the OD obtained for the negative control, milk). Despite the negative selection on PAI-1, 375 of these 377 VHHs recognized PAI-1 as well as PN-1. The two clones specific for PN-1 (KB-PN1-01 and KB-PN1-02) were expressed in *E coli* Shuffle cells and purified for further characterization.

Kinetic analysis of the interaction between the VHHs and hPN-1, mPN-1, and hPAI-1 were analyzed by biolayer interferometry. Both VHHs displayed efficient binding to hPN-1 with maximal binding being 4.9 ± 0.1 nm and 5.1 ± 0.1 nm for KB-PN1-01 and KB-PN1-02, respectively (Figure 1B). Binding to mPN-1 was less efficient with maximal binding being 2.0 ± 0.1 nm and 1.9 ± 0.1 nm, respectively. Only low binding was observed for PAI-1 (maximal binding 0.6 ± 0.2 and 0.6 ± 0.1 nm). Three bivalents variants were engineered, designated KB-PN1-01bv, KB-PN1-02bv, and KB-PN1-0102. We next analyzed the capacity of the different VHHs to inhibit PN-1 by measuring restoration of thrombin activity. As expected, in the presence of hPN-1 or mPN-1, thrombin activity was strongly decreased with a residual thrombin activity of 5 ± 2% for hPN-1 and 2 ± 1% for mPN-1 (Figure 1C). Among the different VHHs, only KB-PN1-01 was able to partially neutralize hPN-1 and mPN-1, restoring residual thrombin activity to 31 ± 5% for hPN-1 and 13 ± 1% for mPN-1, respectively (Figure 1C). All other VHH variants proved unable to inhibit hPN-1 or mPN-1 (Figure 1C). Thus, despite the identification of VHHs specific for PN-1, these variants were unfortunately unable to efficiently inhibit its action towards thrombin.

3.2 | Developing anti-PN-1 VHHs from a synthetic VHH library

To obtain specific potent inhibitory anti-PN-1 VHHs, we next moved to a synthetic VHH library.[27] The VHH were selected using the same protocol used for classical VHHs. The four strongest binders were selected for further characterization: H12, B11, F06, and A08, whose sequences are indicated in Figure 2A. The hPN-1, mPN-1, and PAI-1 nonadsorbed phage ELISA presented in Figure 2B highlights the distinct recognition of all four VHHs for hPN-1 and mPN-1 as well as their non-recognition of hPAI-1.

3.3 | Characterization of anti-PN-1 VHHs obtained from the synthetic library

The purified VHHs were analyzed for their interaction with PAI-1 and both hPN-1 and mPN-1. In line with the initial screening, none of the 4 selected VHH displayed relevant binding to human or murine PAI-1 (Figure 3A-B). In contrast, VHHs H12, B11, F06, and A08 all displayed dose-dependent binding to both human and murine PN-1 (Figure 3C-D). To assess the inhibitory activity of the different VHHs toward PN-1, we next performed an assay measuring thrombin activity in the presence of PN-1 and the various VHHs. Although being most efficient in binding to both hPN-1 and mPN-1, VHH H12 interfered only partially with PN-1-mediated inhibition of thrombin activity, restoring thrombin activity to 74 ± 5% and 53 ± 17% for hPN-1 and mPN-1, respectively (Figure 3E-F). VHHs B11, F06, and A08 proved more efficient in lifting hPN-1 inhibition of thrombin, with a recovery of thrombin activity of 100 ± 7% for B11, 100 ± 5% for F06, and 100 ± 11% for A08 (Figure 3E). A similar potent inhibitory capacity was also observed for mPN-1:92 ± 10% for B11, 96 ± 9% for F06, and 94 ± 14% for A08 (Figure 3F). None of these VHHs affected inhibition of u-PA by PAI-1 (Figure 3G). In conclusion, this second selection strategy did generate VHHs being selective and inhibitory towards both hPN-1 and mPN-1.

3.4 | Determination of the IC50 for B11, F06, and A08 VHHs

To determine the IC50 of B11, F06, and A08 toward hPN-1 and mPN-1, we incubated various concentrations of VHHs with 10 nmol/L PN-1 and 1 nmol/L thrombin. The degradation of PNAPEP-0238 substrate was followed for 2 hours. The calculated IC50 values for the tested VHHs toward hPN-1 were 0.05 ± 0.01 μmol/L for B11, 0.29 ± 0.03 μmol/L for F06, and 0.96 ± 0.39 μmol/L for A08 (Figure 4A). Using mPN-1, the respective calculated values of IC50 were 1.58 ± 0.24 μmol/L for B11, 0.56 ± 0.13 μmol/L for F06, and 2.88 ± 0.77 μmol/L for A08 (Figure 4A). To increase the inhibitory effect of the VHHs especially toward mPN-1, we next generated three different bivalent constructs, B11bv, B11F06, and B11A08 (Figure 4B). Following this engineering step, we verified whether the purified bivalent VHHs had kept their ability to bind hPN-1 and mPN-1 (Figure 5A-B). We also confirmed that they still did not recognize PAI-1 (not shown).

The IC50 of the bivalent VHHs were markedly improved compared with monovalent VHHs with values of 41 ± 7 nmol/L for B11bv, 62 ± 6 nmol/L for B11F06, and 142 ± 28 nmol/L for B11A08 toward hPN-1. For mPN-1, the IC50s were also improved with values of 825 ± 9 nmol/L, 414 ± 141 nmol/L, and 524 ± 174 nmol/L for B11bv, B11F06, and B11A08, respectively (Figure 5C).

In an attempt to identify the binding region of the VHHs on PN-1, we performed BLI-analysis to test the interaction between a peptide covering the RCL region of PN-1 (either intact or after cleavage by thrombin) and the bivalent VHHs. All three bivalent sdAbs bound efficiently to the RCL peptide, demonstrating that they are directed against this area of the protein (Figure 5D). Binding to this peptide was strongly reduced for each bivalent construct upon RCL cleavage by thrombin. These data are compatible with VHH B11 binding to the C-terminal portion of the RCL (which is released from the sensor after thrombin cleavage) or to an epitope overlapping the P1-P′1 cleavage site. None of the VHHs appear to recognize the N-terminal portion of the RCL (which remains bound to the sensor after thrombin cleavage). The data do not distinguish between F06 and A08 binding to the C-terminal portion of the RCL or to an epitope outside the RCL.

3.5 | Effect of bivalent VHHs on in vitro coagulation assays

To test the effect of bivalent VHHs on coagulation, we performed modified PT and aPTT coagulation assays with mPN-1 using murine plasma.

First, a PT was developed using wild-type plasma incubated with a prothrombin-deficient lyophilized plasma to be able to use only small quantities of mPN-1. Using this modified assay, PT was 69.0 ± 2.4 seconds and increased to 123.8 ± 6.6 seconds after addition of 62.5 nmol/L mPN-1 (Figure 6A). At a concentration of 288 nmol/L, all three bivalent VHHs were able to restore the PT, while not affecting PT in the absence of added mPN-1 (83.5 ± 1.1 seconds for B11bv; 83.3 ± 1.5 seconds for B11F06; 93.2 ± 4.4 seconds for B11A08). In this assay, B11A08 was slightly less efficient that the other two VHHs.

We also tested the effect of bivalent VHHs in a modified aPTT (Figure 6B). Similar to the PT, we designed specific conditions where aPTT is increased, by using F8-deficient murine plasma to make the test more sensitive to PN-1. aPTT in F8-deficient murine plasma was 97.0 ± 2.7 seconds and increased 1.6-fold to 148.4 ± 7.9 seconds when mPN-1 was added. The three VHHs decreased significantly the aPTT, with B11F06 being most efficient (112.5 ± 7.0 seconds; Figure 6B).

We next investigated whether our bivalent VHHs were also able to inhibit endogenous PN-1 present in platelet alpha granules. For this experiment, supernatant from nonactivated or TRAP-activated

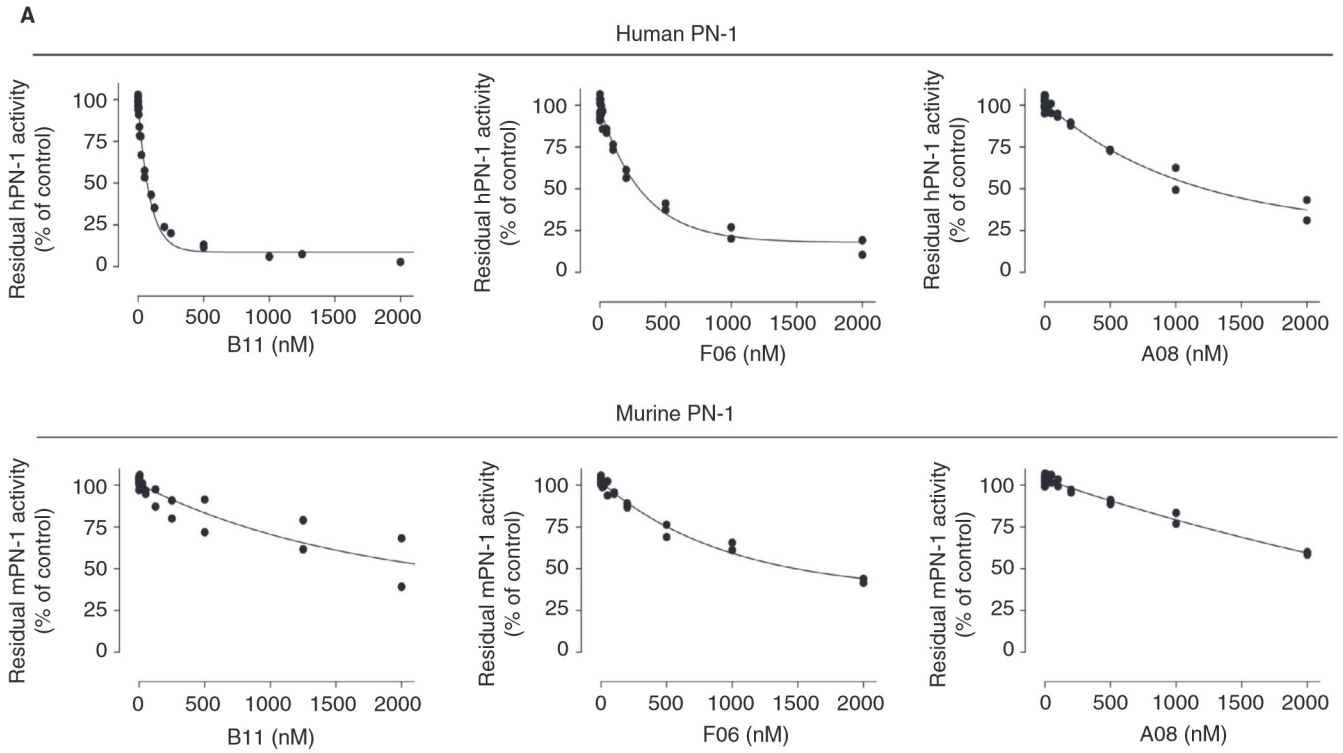

VHHs	B11	F06	A08
nPN-1	0.06±0.01 μM	0.23±0.02 μM	1.17±0.12 μM
mPN-1	1.27±0.46 μM	0.67±0.08 μM	3.54±1.23 μM

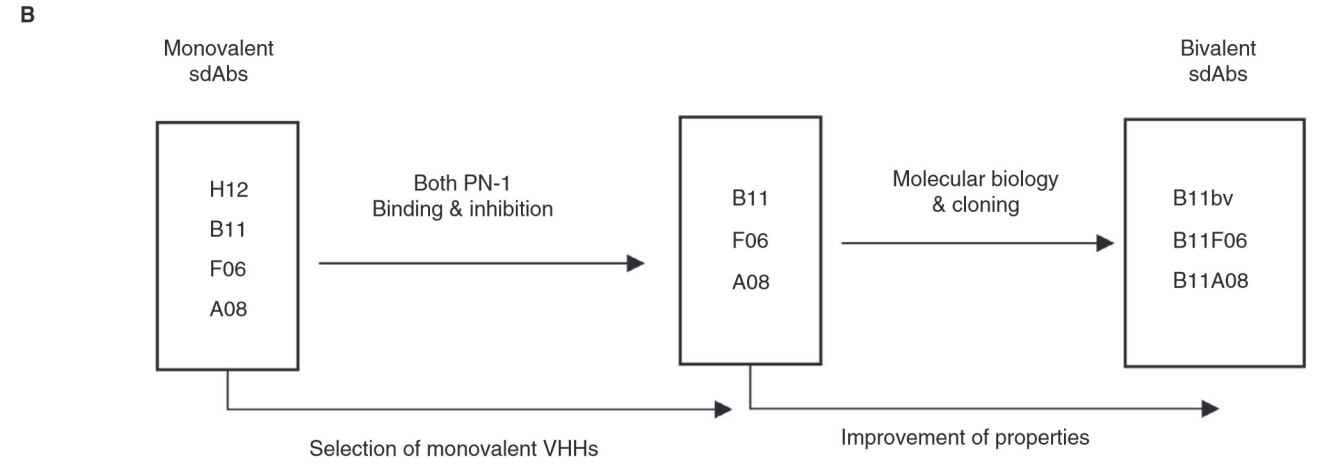

FIGURE 4 Determination of half maximal inhibitory concentration of monovalent VHHs and strategy to identify and improve the best monovalent VHHs. A, hPN-1 or mPN-1 were incubated with different concentrations of monovalent VHHs (0-2 μmol/L) and 1 nmol/L of thrombin was added to each well. Residual thrombin catalytic activity was measured by assaying the rate of PNAPEP-0238-hydrolysis. Data represent residual thrombin activity as percentage of thrombin alone. Each data point represents an individual measurement. The table recapitulates the IC50 obtained for the monovalent VHHs towards mPN-1 and hPN-1 (mean ± SD; n = 3). B, Strategy to select the best monovalent VHHs leading to the choice of bivalent VHHs in order to improve their properties

platelets was used as a source of PN-1. The efficacy of secreted PN-1 in inhibiting thrombin activity was thus investigated. As expected, when supernatant from nonactivated platelets was incubated with thrombin, no inhibitory effect was measured because PN-1 had not been released from platelet α-granules (Figure 6C). In contrast, residual thrombin activity dropped to 18 ± 15% in the presence of

supernatant derived from TRAP-activated platelets (Figure 6D). The bivalent VHHs abolished the inhibition of thrombin activity by the secreted platelet PN-1, thrombin activity being restored to 97 ± 23% for B11bv, 88 ± 21% for B11F06, and 100 ± 15% for B11A08.

4 | DISCUSSION

Many physiological systems use proteins that share structural homologies. One example is the coagulation cascade, in which vitamin K-dependent serine proteases participate as pro- and anti-coagulant enzymes. From an evolutionary perspective, these structurally homologous proteins seem to originate from gene duplications.[28] Such structural homology is also observed in another group of proteins that participates in hemostasis and beyond (ie, serpins). The vast majority of the natural inhibitors of thrombin, the key final effector of the coagulation cascade, are members of the serpin family.[1] Among them is PN-1, encoded by SERPINE2, which has emerged as a crucial player in thrombin regulation. To better understand the importance of PN-1-mediated thrombin inhibition in the diverse in vitro and in vivo experimental models, as well as to potentially develop therapeutic tools, we aimed to generate neutralizing antibodies against PN-1.

The generation of antibodies against PN-1 has been hampered by the fact that there is a large structural and functional homology between PN-1and its nearest phylogenetical family member, PAI-1, a protein encoded by SERPINE1. PN-1 shares 41% homology with PAI-1[2,26,29] and has a target protease specificity overlapping with the one of PAI-1.[6] Such properties have complicated the generation of specific anti-PN-1 antibodies, as illustrated by the cross-reactivity of virtually all commercially available anti-PN-1 antibodies with PAI-1. Therefore, it was within the objectives of this study to design a selection process that would favor the isolation of single-domain antibodies that bind and inhibit PN-1 but leave PAI-1 unaffected.

In a first series of experiments, we selected VHHs against PN-1 after phage-display screening using a llama library, obtained after immunization with both hPN-1 and mPN-1. Despite the negative selection using PAI-1 coated beads, only two of 377 selected clones proved specific for PN-1, with minimal binding to PAI-1. These data suggest that negative preselection of phages may indeed result in VHHs that have improved specificity, although the efficacy of this approach remains weak. Unfortunately, none of the two PN-1 specific clones, designated KB-PN1-01 and KB-PN1-02, displayed sufficient inhibitory activity toward hPN-1 and mPN-1. Although these VHHs may find use in other types of applications (eg. as reagents for flow cytometry, ELISA, Western blots, or immunofluorescence), an additional search was needed to obtain inhibitory VHHs.

The lack of sufficient numbers of PN-1-specific VHHs may originate from different possibilities: first, the majority of PN-1 peptides exposed for antibody generation in the llama overlap to a large extent with similar epitopes in PAI-1; second, PN-1 is a rather non-immunogenic protein, reducing the immunogenic response during the immunization process; third, the final size of the llama-derived library is too small to obtain sufficient numbers of PN-1-specific VHHs, and an extended diversity of the library would be needed. A second series of screening was therefore performed using a unique humanized VHH synthetic antibody library coding for 3×10^9 VHHs (ie, 30-fold more diverse than the llama-derived library).[27] This synthetic library was designed to produce stable, high-affinity binders without the need for animal immunization.

The use of the synthetic naïve library appeared to be successful because four VHHs were identified that were not only specific to hPN-1 and mPN-1, with no detectable binding to PAI-1, but also having strong inhibitory activity toward PN-1. These VHHs were named H12, B11, F06, and A08. B11, F06, and A08 were able to fully neutralize PN-1 in thrombin-based activity assays, whereas H12 displayed partially inhibitory activity. The analysis of their sequences revealed a relatively conserved CDR-2 for H12, B11, and F06, whereas no consensus sequences were present in CDR-1 and CDR-3, apart from being enriched in hydrophilic amino acids (Figure 2). The most important variability between these four VHHs was found in the CDR-3, with lengths varying from nine residues for H12 and A08 to 15 and 18 residues for F06 and B11, respectively (Figure 2). The presence of a long CDR-3 sequence is often seen in the VHHs and allows enlarging the contact surface of the antibody fragment with the antigen. However, we could not observe a clear correlation between CDR-3 size and affinity because the H12 and B11 (having the shortest and longest CDR-3, respectively) displayed more efficient binding to hPN-1 compared with F06 and A08 (Figure 3). In contrast, B11 and F06 were more efficient than H12 and A08 in neutralizing PN-1 activity toward thrombin, suggesting that the larger antigen-binding surface contributes to the interference with PN-1/thrombin interactions.

We noticed that the monovalent VHHs were relatively weak inhibitors of PN-1, with IC50 values varying between 50 and 960 nmol/L. By generating a series of bivalent and bi-paratopic variants, we anticipated to increase the inhibitory potential of these VHHs. Whereas a modest effect was observed on the IC50 between B11 and B11bv with regard to hPN-1, this value was reduced 2-fold for mPN-1 (Figures 4A and 5C). Reductions in IC50 values varying

FIGURE 5 Characterization of bivalent VHHs. A-B, Wells were coated with 0.5 μg of human (A) or murine PN-1 (B) and incubated with different concentrations of bivalent VHHs (0.3-20 μg/mL). Bound VHHs were probed with peroxidase-labeled pAb 6XHis tag. C, hPN-1 or mPN-1 (10 nmol/L) were incubated with different concentrations of bivalent VHHs (0-2000 nmol/L) and 1 nmol/L of thrombin was added to each well. Residual thrombin catalytic activity was measured by measuring the rate of PNAPEP-0238-hydrolysis. Data represent residual thrombin activity as percentage of thrombin alone. Each data point represents an individual measurement. The table recapitulates the IC50 obtained for the bivalent VHHs toward mPN-1 and hPN-1 (mean ± SD; n = 3). D, Representative BLI-analysis graphs (Octet) of VHH binding (100 μg/mL) to biotinylated peptides encompassing the RCL (50 μg/mL). Immobilized peptides were incubated in the absence (red curve) or presence (blue curve) of thrombin (5 U/mL) for 30 min at 37°C before exposure to VHHs. The black curve corresponds to the negative control. Results are expressed as the wavelength shift (in nm) generated by the binding of the different molecules

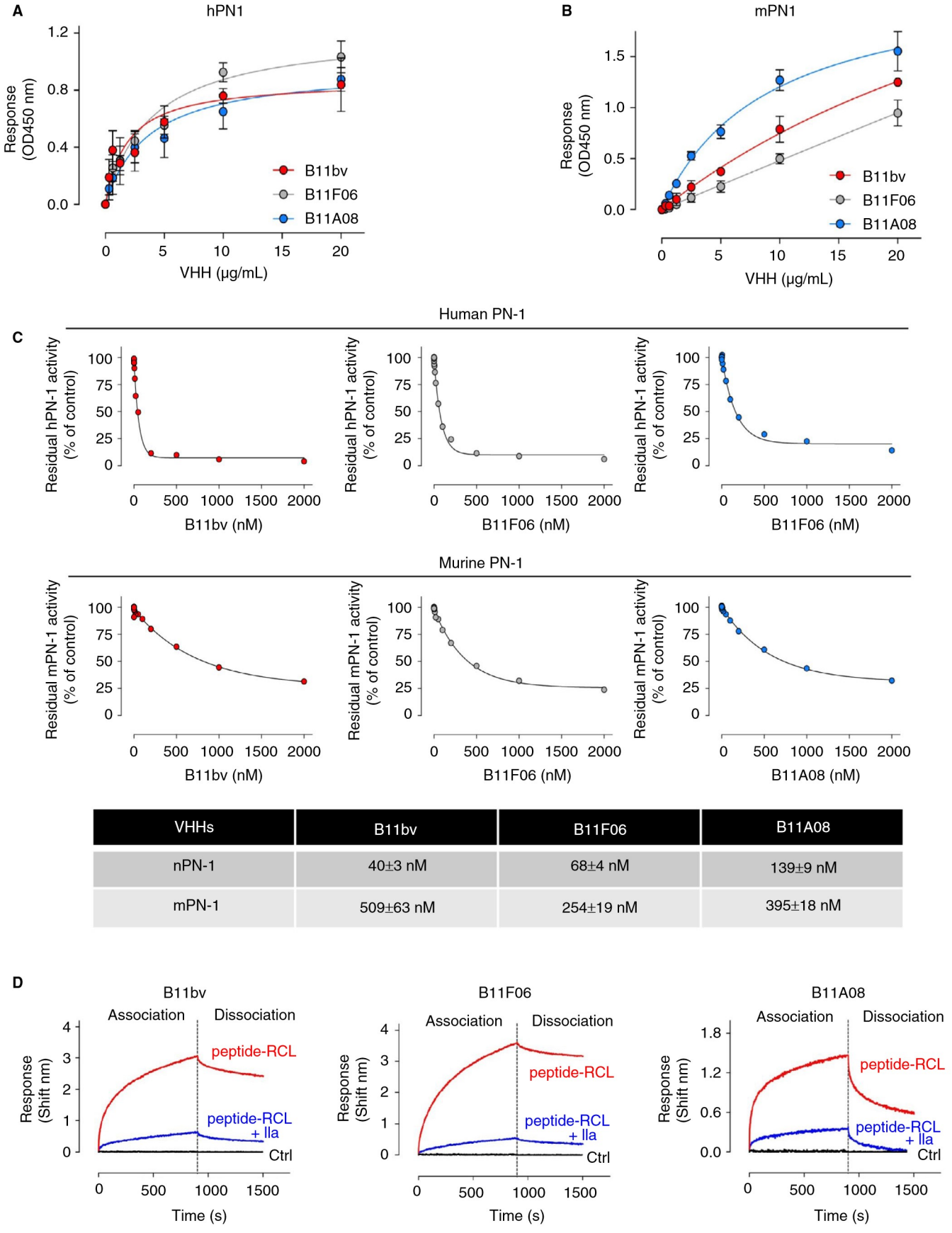

VHHs	B11bv	B11F06	B11A08
nPN-1	40±3 nM	68±4 nM	139±9 nM
mPN-1	509±63 nM	254±19 nM	395±18 nM

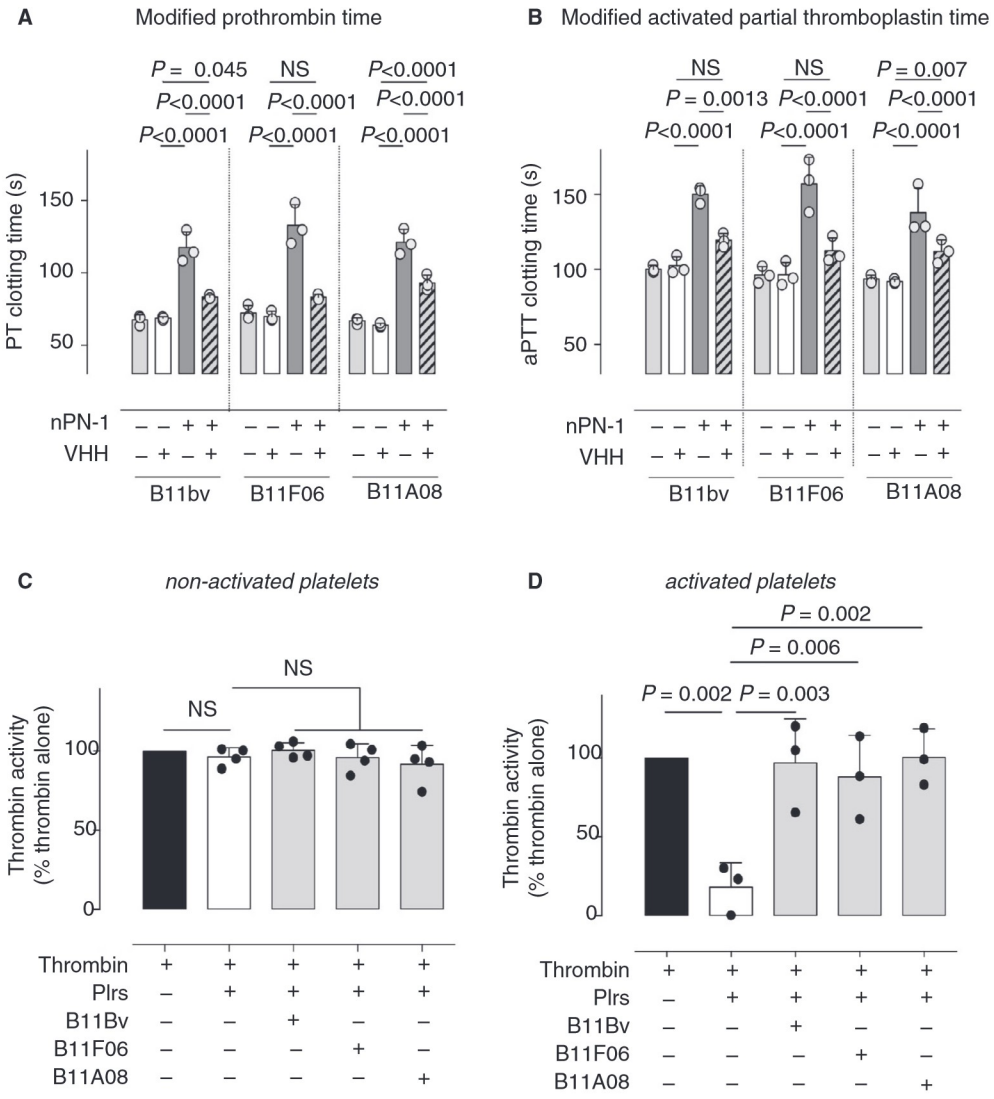

FIGURE 6 Ex vivo experiments with bivalent VHHs. A, Diluted murine wild-type plasma was incubated with 62.5 nmol/L of mPN-1 and spiked with 288 nmol/L of bivalent VHHs and prothrombin time (PT) was measured. B, Diluted FVIII-deficient murine plasma was incubated with 500 nmol/L of mPN-1 and spiked with 625 nmol/L of bivalent VHHs and a modified activated partial thromboplastin time (aPTT) was performed. C-D, 0.1 nmol/L of thrombin was incubated with supernatant derived from nonactivated (C) or TRAP-activated (D) platelets (5×10^8 cells/mL) in the presence or absence of 1 μmol/L bivalent VHHs. Residual thrombin catalytic activity was measured by the rate of PNAPEP 0238-hydrolysis. Data (mean ± SD; n = 3-4) represent residual thrombin activity as percentage of thrombin alone

between 4- and 7-fold were also observed for both other combinations (B11F06 and B11A08) with regard to hPN-1. Moreover, a significant 5-fold reduction of the IC50 was obtained for B11A08, with regard to mPN-1. One would anticipate that the presence of B11 plays a major role in increasing the affinity for hPN-1 when combined with F06 and A08 as well as for mPN-1 when combined with A08 (Figures 4A and 5C). This suggests an additive effect of the presence of both VHHs in the inhibition of PN-1.

Given the inhibitory activity of the VHHs, we explored the possibility that the respective epitopes of the VHHs were located within the RCL sequence of PN-1. Indeed, each of the VHHs was able to bind to an immobilized biotinylated peptide encompassing the RCL sequence (Figure 5D). Moreover, binding virtually disappeared following proteolysis of the peptide by thrombin, which releases the C-terminal portion of the peptide. It seems plausible that the VHHs recognize an epitope around or C-terminal to the thrombin-cleavage site. Most likely, this would represent a linear epitope. The location of this epitope is in agreement with the inhibitory activity of the VHHs because they would directly compete with thrombin for binding to the RCL. In addition, it is worth noting that in contrast to the remainder of the proteins, the RCL sequences of PAI-1 and PN-1 (residues P9-P′9) share <40% identity, which could explain the specificity for PN-1 over PAI-1. Finally, the RCL is a rather flexible structure, and consequently, the VHHs may not recognize all of the conformations that this flexible structure can adopt. This might potentially explain why the monovalent VHHs are relatively weak inhibitors.

To further validate the utility of these VHHs, they were tested under more complex conditions (ie, in plasma rather than a system

using purified proteins). Because PN-1 is absent in plasma, spiking experiments were performed in which mPN-1 was added to murine FVIII-deficient plasma. In both the aPTT and PT assays, final molar concentrations of PN-1 were 2.2- and 22-fold below that of antithrombin, the main thrombin inhibitor in plasma. The notion that the clotting times were prolonged indicates that PN-1 actively inhibits thrombin under these conditions, and is thus able to act in parallel to other anticoagulant proteins such as antithrombin. Moreover, the observation that the VHHs in turn neutralized the effect of PN-1 may suggest that the VHHs display little if any cross-reactivity with other proteins present in plasma. Further, we have previously shown that platelets release PN-1 following their activation, and that this PN-1 impairs the generation of thrombin. Indeed, by using supernatants of nonactivated and TRAP-activated platelets, we could confirm the release of a thrombin-inhibitory molecule (Figure 6C-D). Interestingly, this inhibitory effect could be neutralized by the addition of VHHs, demonstrating that they are able to interact with and inhibit PN-1 that is released from platelets.

Altogether, we have developed a strategy for the development of inhibitory VHHs targeting PN-1, which do not cross-react with PAI-1. These VHHs can be used as research tools to better understand the role of PN-1 in physiological and pathological processes. In addition, they may be explored for their potential therapeutic application in hemophilia treatment for instance.

ACKNOWLEDGMENTS

The study received financial support from the Agence Nationale de la Recherche (ANR-14-OHRI-0013) (M.-C.B. and C.V.D.) and from the Société Française d'Hématologie (SFH) (S.F.).

CONFLICT OF INTEREST

Drs. Christophe, Lenting, Bouton, and Denis are inventors on a patent application regarding single-domain antibodies against protease nexin-1. The other authors have no relevant conflict of interest to declare.

AUTHOR CONTRIBUTIONS

Charlotte Kawecki, Karen Aymonnier, Laurence Venisse, and Véronique Arocas performed experiments and analyzed data. Oliver D. Christophe, Marie-Christine Bouton, Yacine Boulaftali, Peter J. Lenting, and Cécile V. Denis conceived and supervised the study. Charlotte Kawecki, Peter J. Lenting, Marie-Christine Bouton, and Cécile V. Denis wrote the manuscript. All authors contributed to the editing of the final manuscript.

ORCID

Charlotte Kawecki https://orcid.org/0000-0001-9126-6127
Karen Aymonnier https://orcid.org/0000-0002-9587-8822
Véronique Arocas https://orcid.org/0000-0002-2872-8058
Yacine Boulaftali https://orcid.org/0000-0003-4870-2098
Olivier D. Christophe https://orcid.org/0000-0002-9080-6336
Peter J. Lenting https://orcid.org/0000-0002-7937-3429
Marie-Christine Bouton https://orcid.org/0000-0001-5092-7363
Cécile V. Denis https://orcid.org/0000-0001-5152-9156

TWITTER

Cécile V. Denis @cecile_denis

REFERENCES

1. Huntington JA. Serpin structure, function and dysfunction. *J Thromb Haemost*. 2011;9(Suppl 1):26-34.
2. McGrogan M, Kennedy J, Ping Li M, et al. Molecular cloning and expression of two forms of human protease nexin I. *Nat Biotechnol*. 1988;6:172-177.
3. Bouton MC, Boulaftali Y, Richard B, Arocas V, Michel JB, Jandrot-Perrus M. Emerging role of serpinE2/protease nexin-1 in hemostasis and vascular biology. *Blood*. 2012;119:2452-2457.
4. Boulaftali Y, Venisse L, Richard B, et al. Anticoagulant and antithrombotic properties of platelet protease nexin-1. *Blood*. 2010;115:97-106.
5. Evans DL, McGrogan M, Scott RW, Carrell RW. Protease specificity and heparin binding and activation of recombinant protease nexin I. *J Biol Chem*. 1991;266:22307-22312.
6. Scott RW, Bergman BL, Bajpai A, et al. Protease nexin. Properties and a modified purification procedure. *J Biol Chem*. 1985;260:7029-7034.
7. Knauer DJ, Majumdar D, Fong PC, Knauer MF. SERPIN regulation of factor XIa. The novel observation that protease nexin 1 in the presence of heparin is a more potent inhibitor of factor XIa than C1 inhibitor. *J Biol Chem*. 2000;275:37340-37346.
8. Hermans JM, Stone SR. Interaction of activated protein C with serpins. *Biochem J*. 1993;295(Pt 1):239-245.
9. Muhl L, Nykjaer A, Wygrecka M, Monard D, Preissner KT, Kanse SM. Inhibition of PDGF-BB by factor VII-activating protease (FSAP) is neutralized by protease nexin-1, and the FSAP-inhibitor complexes are internalized via LRP. *Biochem J*. 2007;404:191-196.
10. Boulaftali Y, Ho-Tin-Noe B, Pena A, et al. Platelet protease nexin-1, a serpin that strongly influences fibrinolysis and thrombolysis. *Circulation*. 2011;123:1326-1334.
11. Aymonnier K, Kawecki C, Venisse L, et al. Targeting protease nexin-1, a natural anticoagulant serpin, to control bleeding and improve hemostasis in hemophilia. *Blood*. 2019;134:1632-1644.
12. Pasi KJ, Rangarajan S, Georgiev P, et al. Targeting of antithrombin in hemophilia A or B with RNAi therapy. *N Engl J Med*. 2017;377:819-828.
13. Eichler H, Angchaisuksiri P, Kavakli K, et al. Concizumab restores thrombin generation potential in patients with haemophilia: pharmacokinetic/pharmacodynamic modelling results of concizumab phase 1/1b data. *Haemophilia*. 2019;25:60-66.
14. Polderdijk SGI, Baglin TP, Huntington JA. Targeting activated protein C to treat hemophilia. *Curr Opin Hematol*. 2017;24:446-452.
15. Muyldermans S, Atarhouch T, Saldanha J, Barbosa JA, Hamers R. Sequence and structure of VH domain from naturally occurring camel heavy chain immunoglobulins lacking light chains. *Protein Eng*. 1994;7:1129-1135.
16. Muyldermans S. Single domain camel antibodies: current status. *J Biotechnol*. 2001;74:277-302.
17. De Meyer T, Muyldermans S, Depicker A. Nanobody-based products as research and diagnostic tools. *Trends Biotechnol*. 2014;32:263-270.
18. Smolarek D, Bertrand O, Czerwinski M. Variable fragments of heavy chain antibodies (VHHs): a new magic bullet molecule of medicine? *Postepy Hig Med Dosw (Online)*. 2012;66:348-358.
19. Vu KB, Ghahroudi MA, Wyns L, Muyldermans S. Comparison of llama VH sequences from conventional and heavy chain antibodies. *Mol Immunol*. 1997;34:1121-1131.
20. Selbonne S, Azibani F, Iatmanen S, et al. In vitro and in vivo anti-angiogenic properties of the serpin protease nexin-1. *Mol Cell Biol*. 2012;32:1496-1505.

21. Bezeaud A, Denninger MH, Guillin MC. Interaction of human alpha-thrombin and gamma-thrombin with antithrombin III, protein C and thrombomodulin. *Eur J Biochem*. 1985;153:491-496.
22. Aymé G, Adam F, Legendre P, et al. A novel single-domain antibody against von Willebrand factor A1 domain resolves leukocyte recruitment and vascular leakage during inflammation-brief report. *Arterioscler Thromb Vasc Biol*. 2017;37:1736-1740.
23. Behar G, Sibéril S, Groulet A, et al. Isolation and characterization of anti-FcgammaRIII (CD16) llama single-domain antibodies that activate natural killer cells. *Protein Eng Des Sel*. 2008;21:1-10.
24. Barbon E, Ayme G, Mohamadi A, et al. Single-domain antibodies targeting antithrombin reduce bleeding in hemophilic mice with or without inhibitors. *EMBO Mol Med*. 2020;12:e11298.
25. Hoogenboom HR, Griffiths AD, Johnson KS, Chiswell DJ, Hudson P, Winter G. Multi-subunit proteins on the surface of filamentous phage: methodologies for displaying antibody (Fab) heavy and light chains. *Nucleic Acids Res*. 1991;19:4133-4137.
26. Irving JA, Pike RN, Lesk AM, Whisstock JC. Phylogeny of the serpin superfamily: implications of patterns of amino acid conservation for structure and function. *Genome Res*. 2000;10:1845-1864.
27. Moutel S, Bery N, Bernard V, et al. NaLi-H1: a universal synthetic library of humanized nanobodies providing highly functional antibodies and intrabodies. *eLife*. 2016;5:16228.
28. Davidson CJ, Tuddenham EG, McVey JH. 450 million years of hemostasis. *J Thromb Haemost*. 2003;1:1487-1494.
29. Sommer J, Gloor SM, Rovelli GF, et al. cDNA sequence coding for a rat glia-derived nexin and its homology to members of the serpin superfamily. *Biochemistry*. 1987;26:6407-6410.

How to cite this article: Kawecki C, Aymonnier K, Ferrière S, et al. Development and characterization of single-domain antibodies neutralizing protease nexin-1 as tools to increase thrombin generation. *J Thromb Haemost*. 2020;18:2155–2168. https://doi.org/10.1111/jth.14940